5790–5799 *Nucleic Acids Research, 2006, Vol. 34, No. 20* *Published online 19 October 2006*
doi:10.1093/nar/gkl736

Structural diversity of target-specific homopyrimidine peptide nucleic acid–dsDNA complexes

Thomas Bentin, Georg I. Hansen and Peter E. Nielsen*

Department of Medical Biochemistry and Genetics, The Panum Institute, University of Copenhagen, Blegdamsvej 3, 2200 Copenhagen N, Denmark

Received June 15, 2006; Revised August 25, 2006; Accepted September 22, 2006

ABSTRACT

Sequence-selective recognition of double-stranded (ds) DNA by homopyrimidine peptide nucleic acid (PNA) oligomers can occur by major groove triplex binding or by helix invasion via triplex P-loop formation. We have compared the binding of a decamer, a dodecamer and a pentadecamer thymine–cytosine homopyrimidine PNA oligomer to a sequence complementary homopurine target in duplex DNA using gel-shift and chemical probing analyses. We find that all three PNAs form stable triplex invasion complexes, and also conventional triplexes with the dsDNA target. Triplexes form with much faster kinetics than invasion complexes and prevail at lower PNA concentrations and at shorter incubation times. Furthermore, increasing the ionic strength strongly favour triplex formation over invasion as the latter is severely inhibited by cations. Whereas a single triplex invasion complex is formed with the decameric PNA, two structurally different target-specific invasion complexes were characterized for the dodecameric PNA and more than five for the pentadecameric PNA. Finally, it is shown that isolated triplex complexes can be converted to specific invasion complexes without dissociation of the Hoogsteen base-paired triplex PNA. These results demonstrate a clear example of a 'triplex first' mechanism for PNA helix invasion.

INTRODUCTION

Efficient and specific targeting of predefined chromosomal DNA sequences by synthetic ligands is a major goal in chemical biology. A variety of agents are available for this purpose including engineered zinc finger proteins (1), synthetic polyamides (2) triplex forming oligonucleotides (TFOs) (3,4) and peptide nucleic acids (PNAs) (5,6). PNA oligomers are synthetic DNA mimics containing a pseudopeptide backbone consisting of an *N*-aminoethyl glycine polymer to which the nucleobases are connected via methylene carbonyl linkers (7). PNA binds sequence complementary single-stranded nucleic acid targets with high affinity and selectivity (8). Particularly stable 'P-loop' triplex invasion structures can form upon binding of homopyrimidine PNAs to double-stranded (ds) DNA containing a sequence complementary purine target via formation of an internal PNA–DNA–PNA triplex involving combined Watson–Crick and Hoogsteen base pairing (9). In this four-stranded structure, the unbound DNA strand is displaced in a single-stranded conformation. A number of variant P-loop complexes have been described, the formation of which depends on the PNA oligomer and DNA sequence in question (5,6). P-loop complexes have been used in a number of applications for instance for interference with (10–15), or activation of (15–17) transcription.

Because two PNA strands are involved in the triplex invasion P-loop complex, bis-PNA constructs containing two PNA oligomers connected via a flexible linker were generated (18). Bis-PNAs generally bind complementary DNA targets with superior efficiency as compared with conventional 'mono'-PNAs (19,20) because of the pseudo-first-order reaction of binding for bis-PNAs as compared with the pseudo-second order of binding for mono-PNAs. Furthermore, the strand polarity can be optimized for bis-PNAs to allow the preferred parallel (i.e. the PNA N-terminus facing the 5′ end of the bound DNA strand) and anti-parallel (i.e. the PNA N-terminus facing the 3′ end of the bound DNA strand) orientation of the PNA strand bound via Hoogsteen and Watson–Crick base pairs, respectively. The binding can be further enhanced at physiological pH by the substitution of pseudoisocytosine for cytosine (pseudoisocytosine does not require low pH for efficient Hoogsteen base pairing to guanine) (18). Using a mono-PNA the two strands of the P-loop are identical and consequently the polarity of one or the other must be suboptimal unless a symmetrical sequence is targeted. Bis-PNA binding to a cognate target can yield structural isomers of perfectly matched P-loops. Such isomers are the consequence of alternative trajectories

*To whom correspondence should be addressed. Tel: +45 35327762/61; Fax: +45 35396042; Email: pen@imbg.ku.dk

The authors wish it to be known that, in their opinion, the first two authors should be regarded as joint First Authors.

of the bis-PNA linker relative to the DNA strands in kinetically trapped complexes (21).

Because the dissociation rate of triplex invasion complexes is exceedingly slow (19,22) (and often not directly measurable at physiological temperature), helix invasion using decamer homopyrimidine PNA oligomers is kinetically controlled (23). Consequently, single mismatch specificity is also kinetically controlled, i.e. depending on the on-rate only (24). Typically, the association rate for fully matched complexes is significantly higher than that for mismatched complexes. However, once formed, even mismatched complexes remain highly stable so prolonged incubation times or increased PNA concentrations will eventually result in the formation of mismatched complexes (23).

Different mechanisms have been proposed for P-loop formation (23,25,26). Current evidence favour a 'Hoogsteen first' mechanism in which one PNA strand initially binds as a non-invasion triplex in the major groove via Hoogsteen base pairs followed by binding of another PNA strand via helix invasion and Watson–Crick base pairing. The evidence for this mechanism is indirect, however, and the molecular details remain poorly understood.

Clearly, kinetic control is of paramount importance in helix invasion of dsDNA by PNA. Moreover, the extent to which kinetics and thermodynamics each contribute to the control of PNA–dsDNA recognition is most likely shifted further towards kinetics for PNA oligomers of increased length. This is particularly pertinent for targeting unique sequences in the human genome, which from statistical considerations would require recognition of 15–17 bp. We therefore asked what might be the structural consequences of using such extended PNA oligomers for P-loop formation. To avoid the structural and kinetic complications associated with bis-PNAs (see above), we used conventional mono-PNAs. We analysed PNA–dsDNA complexes resulting from incubation of 10mer, 12mer and 15mer homopyrimidine PNAs with dsDNA containing a cognate sequence target. The results show that increased PNA oligomer length causes increased complexity of the generated sequence-targeted complexes. Furthermore, the data reveal the existence of distinct pathways for helix invasion by homopyrimidine PNA.

MATERIALS AND METHODS

PNA oligomers

PNA oligomers were synthesized as described (18,27). Conjugation of the nitrilotetraacetic acid (NTA) group to the N-terminus PNA was previously described (28). The following PNAs were used: PNA1707 (H-TTTTTCTCTC-Lys-NH_2) (measured mass: 2761; calculated mass: 2763), PNA1708 (H-TTTTTCTCTCTC-Lys-NH_2) (measured mass: 3276; calculated mass: 3280), PNA2046 (NTA-Lys-TTTT-TCTCTCTC-Lys-NH_2) (measured mass: 3584; calculated mass: 3583), PNA1940 (NTA-Lys_2-TTTTTCTCTCTCTCT-Lys-NH_2) (measured mass: 4492; calculated mass: 4495). PNA concentrations were determined by spectrophotometry at 260 nm using the following molar extinction coefficients: εT (8800 M^{-1} cm^{-1}) and εC (7300 M^{-1} cm^{-1}). Low binding tubes (Sorenson Biosciences Cat. no. 11720 or Eppendorf Cat. no. 22 43 108-1) and tips (Sorenson Biosciences Cat. no.: 35010 and 35090) were used.

DNA

All DNA manipulations were done using standard methods (29). The p322 vector is a pUC19 derivative containing the PNA target sequence 5′-AAAAAGAGAGAGAGA-3′/5′-TCTCTCTCTCTTTTT-3′) in the polylinker region. The PNA target is flanked on one side by a unique engineered XbaI site and on the other side by an EcoRI restriction site from the vector (see Supplementary Material). The plasmid was propagated in *Escherichia coli* strain XL1-Blue (Stratagene), amplified by maxipreparation (Jet Star, Genomed) and verified by sequencing at DNA Technology, Denmark.

The relevant DNA restriction fragment of p322 was 5′-labelled using polynucleotide kinase and [γ-^{32}P]ATP or 3′-labelled using the Klenow fragment of DNA polymerase and [α-^{32}P]dATP at the desired end as indicated in the figure legends using standard methods (29). The DNA fragments were resolved using 5% polyacrylamide gels (30:1 in acrylamide to bisacrylamide), and the relevant fragment was excised and eluted overnight into 0.5 M ammonium acetate, 1 mM EDTA. Recovered ^{32}P-DNA was precipitated with 96% ethanol, washed with 70% ice-cold ethanol and air dried. The DNA was resuspended in H_2O and stored at −20°C.

Analyses of PNA binding to a target in dsDNA by gel-shift and chemical probing

^{32}P-DNA fragment (10–20 nM) was incubated with the indicated amount of PNA for 1 h in 20 µl of 10 mM sodium phosphate at pH 6 or 6.5 as indicated (slightly acidic due to the requirement of Hoogsteen base pairing on protonization of cytosine position N3) at 37°C. Resulting complexes were resolved by electrophoretic gel-shift analysis using native TAE-buffered 10% PAGE and visualized by autoradiography.

For *in situ* chemical probing with DMS and $KMnO_4$, varying PNA concentrations (0.25–10 µM) were used to establish the desired PNA–dsDNA complexes. Individual PNA–dsDNA complexes were excised from native polyacrylamide gels and processed basically as described (5,21) using optimized *in situ* probing reaction times of 1 min (DMS) or 2 min ($KMnO_4$).

Fe/NTA affinity cleavage was done in 100 µl sodium phosphate buffer. Eight µl of 10 mM $(NH_4)_2[Fe(SO_4)_2]$ was added and incubation continued for 5 min at 37°C followed by addition of 20 µl 50 mM DTT, and incubation for 1 h at 37°C. The reactions were terminated by addition of 10 µl of 0.5 M EDTA at pH 8. Adenine/guanine-specific sequence reactions were performed as described (5).

Kinetic analyses were conducted by setting up a master mix ($V = 220$ µl) containing PNA1940 at a final concentration of 5 µM and ^{32}P-labelled target DNA fragment in 10 mM sodium phosphate (pH 6.5). At the indicated length of time, 20 µl sample was withdrawn, combined with TAE loading buffer and immediately resolved by 10% TAE-buffered PAGE. The data were quantified using a phosphorimager and Image Quant software. When appropriate,

the 'quench' oligonucleotide 5′-dAGAGAGAGAGAAAAA-3′ was added to a 2- to 4-fold molar excess relative to PNA1940.

RESULTS AND DISCUSSION

Gel-shift analysis of PNA–dsDNA complexes

The PNA decamer gave rise to a single gel-shift [Designated PD^{10}—the designation 'PD' identifies a complex as consisting of PNA and dsDNA. To keep track of gel-shifted complexes a suffix is added that includes a roman number identifying the gel-shift complex in question and a superscript identifying the PNA oligomer length used. The nomenclature should not be confused with the 'PD-loop' (30).] upon binding to a dsDNA fragment harbouring one sequence complementary target (Figure 1A). In contrast, incubation of the PNA dodecamer or the PNA pentadecamer with the dsDNA fragment harbouring the sequence complementary target resulted in multiple retarded gel migration species designated PDI^{12}–$PDIII^{12}$ and PDI^{15}–$PDVII^{15}$, respectively (Figures 2A and 3A).

Decamer PNA–dsDNA complexes

P-loop structures can be probed using potassium permanganate ($KMnO_4$) and dimethyl sulphate (DMS) (9). $KMnO_4$ preferentially oxidizes the 5–6 double bond of unstacked (single-stranded) thymine nucleobases, which poises the DNA strand for alkali-induced backbone cleavage at such reacted sites (31). Hypersensitivity towards $KMnO_4$ can thus be used to reveal the single-stranded DNA of a P-loop (9). DMS methylates guanine at the N7 position (and to a much lesser extent adenine at the N3 position) (32). Because the guanine N7 is engaged in Hoogsteen hydrogen bonding, PNA interference with DMS methylation can be used to reveal Hoogsteen base pairing, e.g. during P-loop formation.

Chemical probing of the gel-excised PD^{10} complex revealed protection from DMS methylation of residues G_6, G_8 and G_{10} (Figure 1B) and hypersensitivity towards $KMnO_4$ oxidation of T_1–T_5, T_7 and T_9 (Figure 1C). These results are compatible with a triplex invasion complex containing two PNA strands bound via combined Watson–Crick and Hoogsteen base pairs. Because the DNA lacks G-residues as a reporter for DMS probing in the 5′-target region, we cannot formally rule out alternative modes of

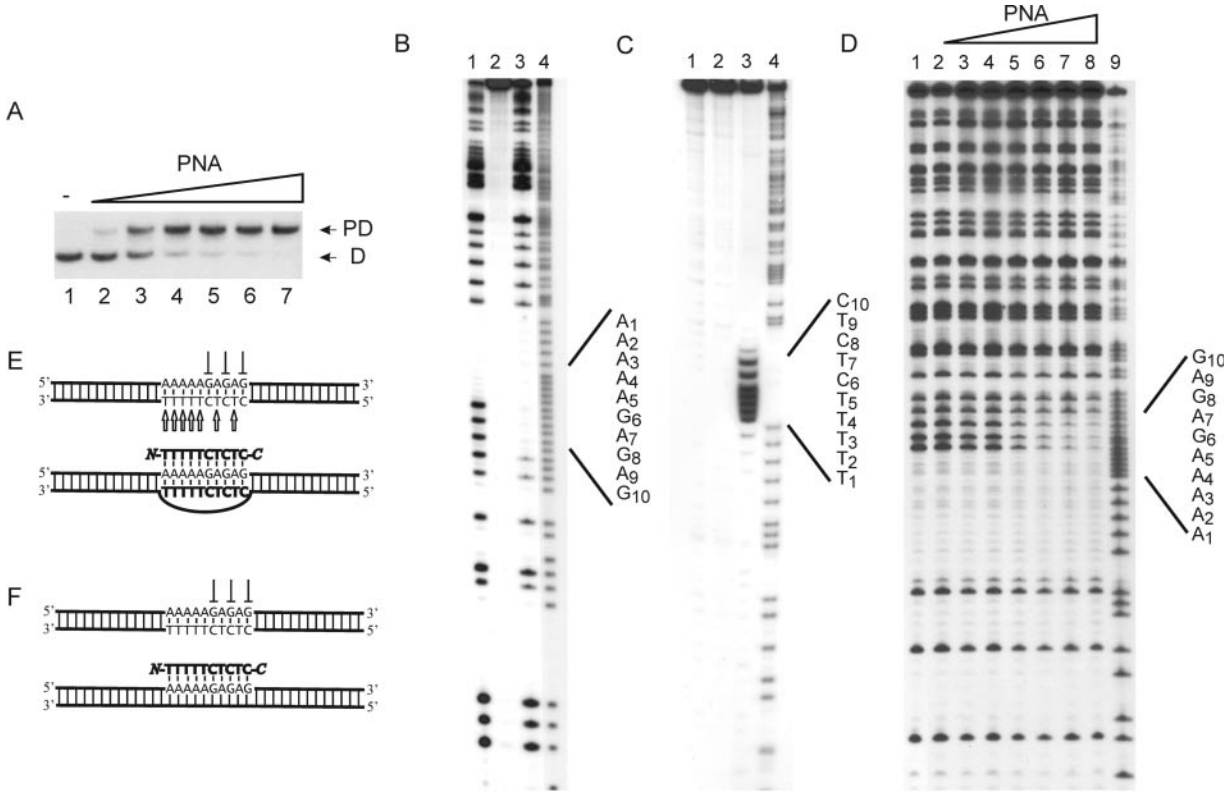

Figure 1. P-loop formation on binding of PNA decamer to dsDNA: (PD^{10}). (**A**) P-loop formation as investigated by gel-shift analysis. P-loops were generated using the following concentrations of PNA 1707: lane 1, w/o PNA; lane 2, 0.25 μM; lane 3, 0.5 μM; lane 4, 0.75 μM; lane 5, 1 μM; lane 6, 2 μM; and lane 7, 4 μM. P-loop (PD) and free dsDNA (D) are indicated. (**B**) *In situ* DMS probing of P-loop complex identified in (A): lane 1, dsDNA + DMS; lane 2, dsDNA w/o DMS; lane 3, PD^{10} + DMS; lane 4, A/G sequence. (**C**) *In situ* permanganate probing of P-loop complex identified in (A): lane 1, DNA + $KMnO_4$; lane 2, DNA w/o $KMnO_4$; lane 3, PD^{10} + $KMnO_4$; and lane 4, A/G sequence. (**D**) DMS probing in solution at elevated high ionic strength (+90 mM KCl) and using the following PNA1707 concentrations: lane 1, w/o PNA; lane 2, 0.13 μM PNA; lane 3, 0.25 μM PNA; lane 4, 0.5 μM PNA; lane 5, 1 μM PNA; lane 6, 2 μM PNA; lane 7, 4 μM PNA; lane 8, 8 μM PNA; and lane 9, A/G sequence. (**E**) Structural assignment as based on the data in (A–C). (**F**) Structural assignment based on the data in (D and manuscript in preparation). We used the 168 bp XbaI–PvuII restriction fragment of p322 either 5′-kinase labeled (A and D) or 3′-Klenow labeled (C) with ^{32}P-phosphate at the XbaI site. The 223 bp PvuII–EcoRI restriction fragment of p322 was 3′-Klenow labeled and used in (B). PNA incubations were at pH 6 as described in Materials and Methods.

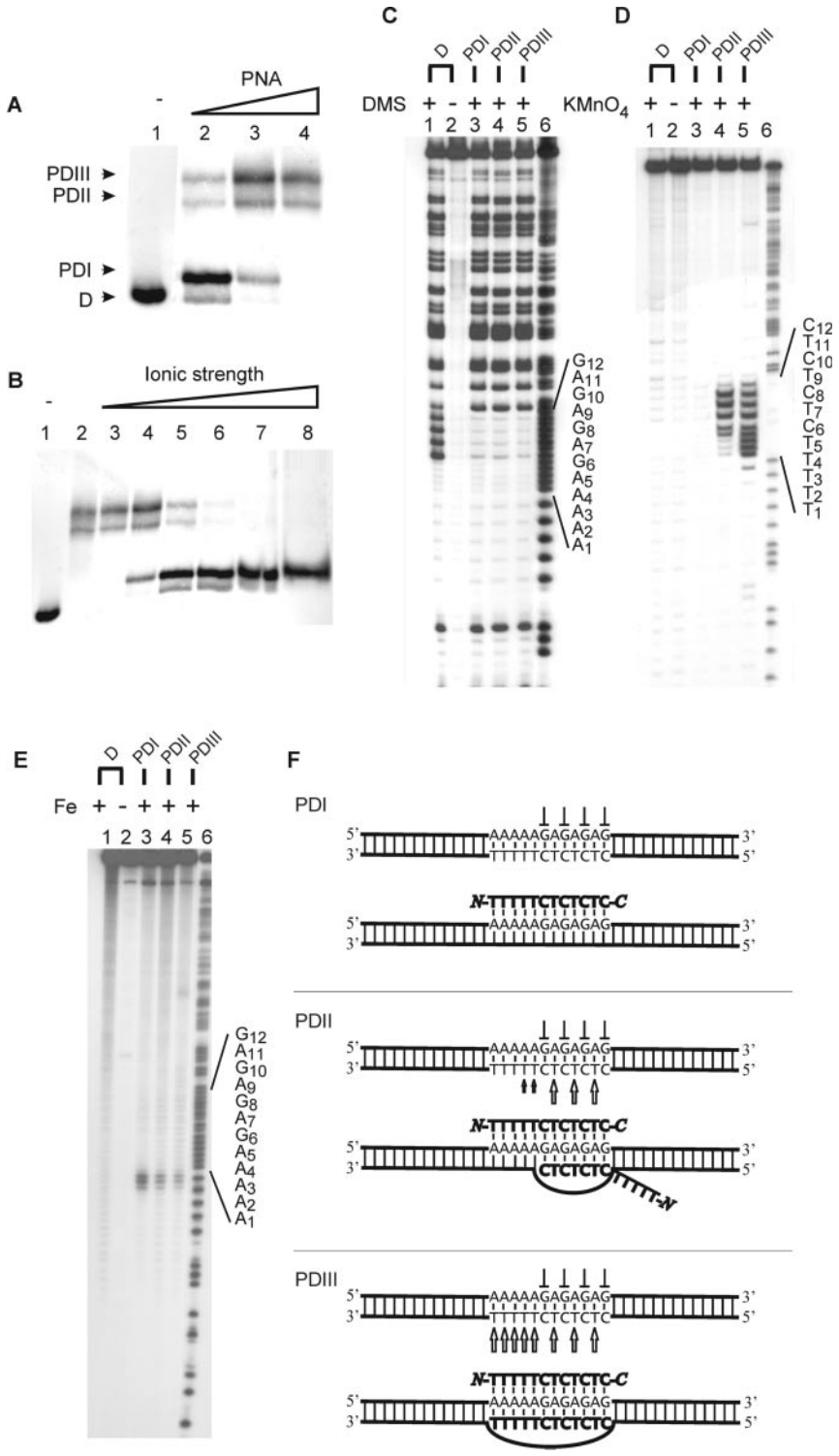

Figure 2. Binding of PNA dodecamer to dsDNA (PD^{12}). Autoradiographs showing binding of the indicated PNAs to dsDNA as investigated by gel-shift analysis (A and B), in situ chemical probing (C and D) and affinity cleavage (E). (**A**) Titration using the following PNA1708 concentrations: lane 1, w/o; lane 2, 0.25 μM; lane 3, 2 μM; and lane 4, 6 μM. Free dsDNA (D) and the formed complexes PDI^{12}, $PDII^{12}$ and $PDIII^{12}$ are indicated. Analogous PD^{12} complexes were obtained using NTA-conjugated PNA2046 (Supplementary Figure S1). (**B**) PD^{12} complex formation as a function of ionic strength using 6 μM PNA1708 and supplemented with the following amounts of KCl: lane 1, w/o; lane 2, 5 mM; lane 3, 10 mM; lane 4, 20 mM; lane 5, 40 mM; lane 6, 80 mM; lane 7, 160 mM; and lane 8, 320 mM. (**C**) DMS probing of gel-purified PD^{12} complexes involving PNA2046: lane 1, dsDNA + DMS; lane 2, dsDNA, w/o DMS; lane 3, PDI^{12} + DMS; lane 4, $PDII^{12}$ + DMS; lane 5, $PDIII^{12}$ + DMS; and lane 6, A/G sequence. (**D**) Permanganate probing of gel-purified PD^{12} complexes involving PNA2046: lane 1, dsDNA + $KMnO_4$; lane 2, dsDNA, w/o $KMnO_4$; lane 3, PDI^{12} + $KMnO_4$; lane 4, $PDII^{12}$ + $KMnO_4$; lane 5, $PDIII^{12}$ + $KMnO_4$; and lane 6, A/G sequence. (**E**) Fe/NTA affinity cleavage of gel-purified PD^{12} complexes involving PNA2046: lane 1, dsDNA + Fe/NTA; lane 2, dsDNA, w/o Fe/NTA; lane 3, PDI^{12} + Fe/NTA; lane 4, $PDII^{12}$ + Fe/NTA; lane 5, $PDIII^{12}$ + Fe/NTA; and lane 6, A/G sequence marker. (**F**) Structural assignment as based on the probing results [arrow ($KMnO_4$ hypersensitivity), perpendicular symbol (DMS protection)]. The 168 bp XbaI–PvuII restriction fragment of p322 was used either 5′-kinase labelled (A–C, E) or 3′-Klenow labelled (D) with ^{32}P-phosphate at the XbaI site. PNA incubations were at pH 6.5 as described in Materials and Methods.

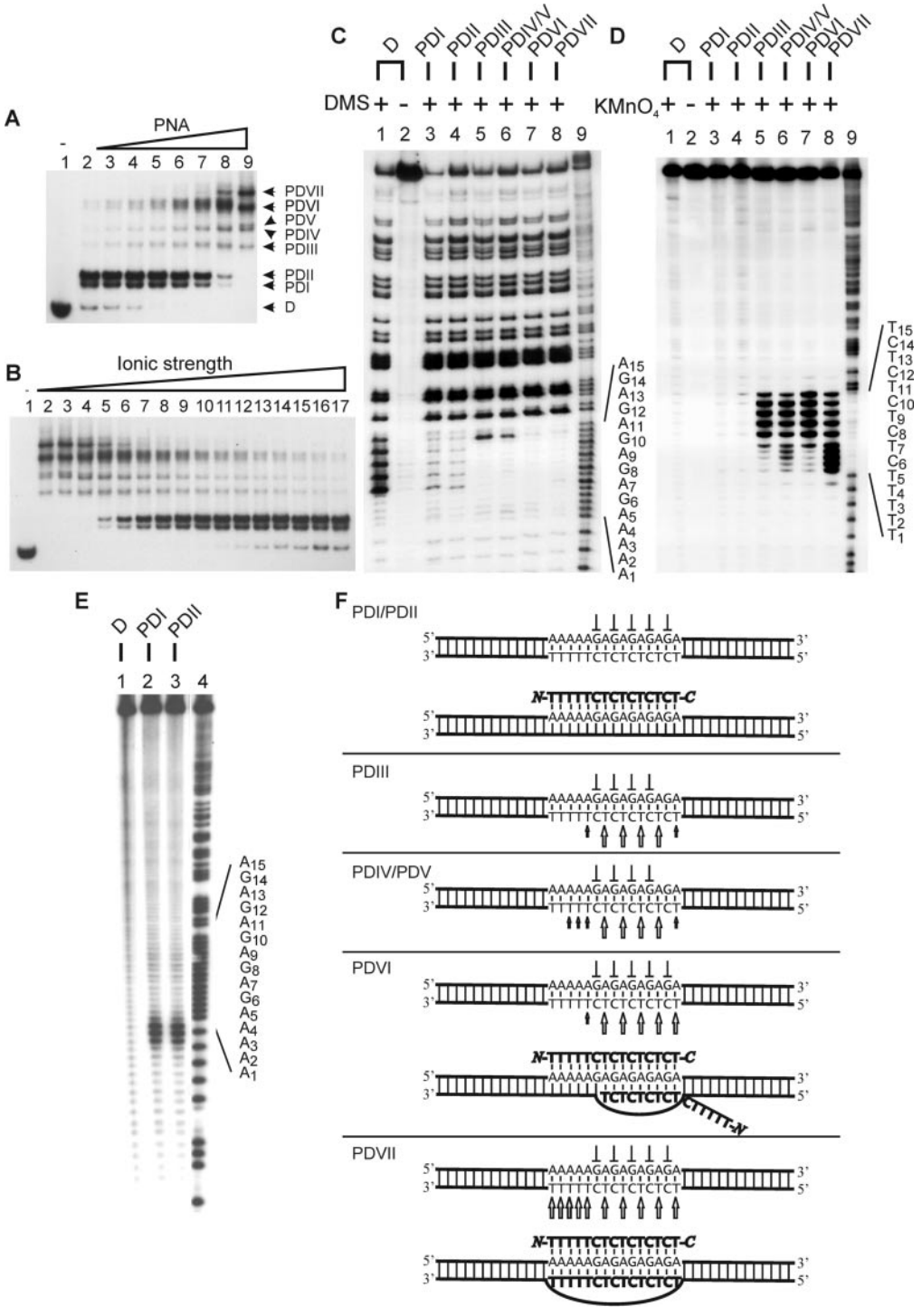

Figure 3. Binding of PNA pentadecamer to dsDNA (PD^{15}). Autoradiographs showing binding of PNA1940 to dsDNA as investigated by gel-shift analysis (A and B), *in situ* chemical probing (C and D) and affinity cleavage (E). (**A**) PNA titration using the following concentrations: lane 1, w/o; lane 2, 0.25 μM; lane 3, 0.5 μM; lane 4, 0.75 μM; lane 5, 1 μM; lane 6, 2 μM; lane 7, 4 μM; and lane 8, 8 μM. Free DNA (D) and the formed complexes PDI^{15}–$PDVII^{15}$ are indicated. (**B**) PD^{15} complex formation as a function of ionic strength. Incubation was carried out using 6 μM PNA and supplemented with KCl as follows: lane 1, w/o; lane 2, 5 mM; lane 3, 10 mM; lane 4, 20 mM; lane 5, 30 mM; lane 6, 40 mM; lane 7, 50 mM; lane 8, 60 mM; lane 9, 70 mM; lane 10, 80 mM; lane 11, 100 mM; lane 12, 120 mM; lane 13, 140 mM; lane 14, 160 mM; lane 15, 180 mM; lane 16, 300 mM; and lane 17, 320 mM. (**C**) DMS probing of the complexes identified in (A). Lane 1, dsDNA + DMS; lane 2, dsDNA w/o DMS; lane 3, PDI^{15} + DMS; lane 4, $PDII^{15}$ + DMS; lane 5, $PDIII^{15}$ + DMS; lane 6, $PDIV^{15}$/PDV^{15} + DMS; lane 7, $PDVI^{15}$ + DMS; lane 8, $PDVII^{15}$ + DMS; and lane 9, A/G sequence marker. (**D**) $KMnO_4$ probing of the complexes identified in (A). Lane 1, dsDNA + $KMnO_4$; lane 2, dsDNA w/o $KMnO_4$; lane 3, PDI^{15} + $KMnO_4$; lane 4, $PDII^{15}$ + $KMnO_4$; lane 5, $PDIII^{15}$ + $KMnO_4$; lane 6, $PDIV^{15}$/PDV^{15} + $KMnO_4$; lane 7, $PDVI^{15}$ + $KMnO_4$; lane 8, $PDVII^{15}$ + $KMnO_4$; and lane 9, A/G sequence marker. (**E**) Autoradiograph showing PDI^{15} and $PDII^{15}$ subjected to Fe/NTA affinity cleavage. Lane 1, dsDNA + Fe/NTA; lane 2, PDI^{15} + Fe/NTA; lane 3, $PDII^{15}$ + Fe/NTA; and lane 4, A/G sequence marker. (**F**) Structural assignment (arrow, $KMnO_4$ hypersensitivity; perpendicular symbol, DMS protection). The 168 bp Xba–PvuII restriction fragment of p322 was used either 5′-kinase labeled (A–C, E) or 3′-Klenow labeled (D) with ^{32}P-phosphate at the XbaI site. PNA incubations were at pH 6.5 as described in Materials and Methods.

binding for the Hoogsteen base-paired PNA strand. However, we favour the parallel alignment shown in Figure 1E because this is the optimal binding orientation (18) and because incomplete base pairing would involve as few as 5 bp of PNA–DNA hybrid that would be very unstable (33).

When the PNA binding reaction was carried out at elevated ionic strength conditions no hybridization of conventional unmodified decamer homopyrimidine PNA was detected in gel-shift analyses. In contrast, probing directly in solution revealed a PNA concentration-dependent protection from DMS methylation in reactions supplemented with 90 mM KCl (Figure 1D). These results [consistent with the previous results (11,24,34–36)], show that invasion by simple PNA oligomers is severely compromised at elevated ionic strength and suggests that a conventional triplex structure involving PNA decamer bound via Hoogsteen base pairs is formed, which is not sufficiently stable for gel-shift analysis (Figure 1F).

Dodecamer PNA–dsDNA complexes

Three complexes designated PDI^{12}, $PDII^{12}$ and $PDIII^{12}$ were identified by gel-shift analysis upon incubation of the PNA dodecamer with the dsDNA fragment containing the cognate sequence target (Figure 2A). The relative ratio of these complexes was PNA concentration dependent. PDI^{12} was the predominant species at low PNA concentrations and the amount of this complex decreased with increasing PNA concentration. In contrast, the amount of $PDII^{12}$ and $PDIII^{12}$ increased with increasing PNA concentration and these complexes were the sole species observed at elevated PNA concentrations.

We anticipated that ionic strength would affect triplex formation much less than helix invasion. Thus to distinguish possible triplex and invasion type complexes, a salt titration was conducted. At the employed PNA concentration, low ionic strength conditions produced only $PDII^{12}$ and $PDIII^{12}$, but as the salt concentration was increased, PDI^{12} emerged at the expense of the former (Figure 2B) suggesting that $PDII^{12}$ and $PDIII^{12}$ are invasion complexes whereas PDI^{12} is a conventional triplex.

To enable an investigation of the PNA strand polarity of gel-shifted complexes, we chose to employ NTA-conjugated PNA oligomers (see below). Using such conjugated dodecamer PNA (PNA2046), gel-shifts PDI^{12}, $PDII^{12}$ and $PDIII^{12}$ were obtained analogously to those obtained with unmodified PNA dodecamer (Supplementary Figure S1).

Chemical probing of gel-excised PDI^{12} involving NTA-conjugated PNA dodecamer, showed that guanine residues G_6 through G_{12} are protected from DMS methylation (Figure 2C, lane 3), and all thymine residues T_1 through T_{11} are resistant to $KMnO_4$ oxidation (Figure 2D, lane 3). These results show PNA binding to residues G_6–G_{12} compatible with a structure containing a single PNA oligomer bound via Hoogsteen base pairs to target residues A_1–G_{12} (since there are no G-residues in the 5′-proximal target, DMS probing cannot be used to reveal PNA binding to this region) (Figure 2F, PDI^{12}).

To investigate the orientation of PNA strands in the generated PD complexes, we employed Fe/NTA affinity cleavage. Ferrous ions are well-known DNA cleaving reagents that function via activation by molecular oxygen. Such reactions are particularly useful in conjunction with a bifunctional molecule containing a DNA-binder linked to a metal chelator because this yields DNA cleavage proximal to the DNA binder (37,38). Lohse *et al.* (28) previously reported the synthesis and properties of such a bifunctional molecule based on a NTA–PNA conjugate in which ferrous iron was chelated to the NTA group.

PDI^{12} subjected to Fe/NTA affinity cleavage showed strand scission 5′-distal to the PNA target (Figure 2E, lane 3). Because the NTA moiety is conjugated via the N-terminus of the PNA (see Materials and Methods), these data are compatible with a parallel orientation of the PNA oligomer and formally establish the binding of the PNA strand to the entire target (residues A_1–G_{12}) (Figure 2F, PDI^{12}).

DMS probing of gel-excised $PDII^{12}$ and $PDIII^{12}$ revealed protection from methylation of guanine residues G_6 through G_{12} (Figure 2C, lanes 4 and 5) similar to that of PDI^{12}. Thus both $PDII^{12}$ and $PDIII^{12}$ contain a PNA strand bound via Hoogsteen base pairs to the target (see below).

Permanganate probing of gel-excised $PDIII^{12}$ revealed hypersensitive thymine residues along the entire target region including T_1–T_{11} (Figure 2D, lane 5). Consequently, the $PDIII^{12}$ complex must constitute a helix invasion type structure in which a Watson–Crick base-paired PNA strand is hybridized to all target residues A_1–G_{12} in a parallel orientation (Figure 2F, $PDIII^{12}$). Permanganate probing of gel-excised $PDII^{12}$ revealed an unequal hypersensitivity of the thymines within the target: T_1 through T_3 were almost entirely resistant to $KMnO_4$ oxidation, T_4 and T_5 showed intermediate $KMnO_4$ hypersensitivity, and finally T_7, T_9 and T_{11} were most hypersensitive (Figure 2D, lane 4). Thus $PDII^{12}$ represent an invasion type structure, with only partial target occupation, in which the helix invasion PNA is bound to DNA target residues G_6–G_{12}. Such partial Watson–Crick base pairing can occur with the optimal anti-parallel strand orientation (Figure 2F, $PDII^{12}$).

Induction of Fe/NTA affinity cleavage in $PDII^{12}$ and $PDIII^{12}$ revealed DNA strand scission 5′ to the PNA target in both cases (Figure 2E, lanes 4 and 5). In $PDII^{12}$, the 5′-cleavage is accounted for by a parallel PNA bound via Hoogsteen base pairs. The PNA strand engaged in Watson–Crick base pairing, is not expected to yield efficient 3′-dsDNA strand scission if the Fe/NTA group is displaced from the target via a segment of unbound PNA (Figure 2F). Finally, in the case of $PDIII^{12}$, selective Fe/NTA affinity cleavage at the 5′-dsDNA target is accounted for by a parallel orientation of both Hoogsteen and Watson–Crick base-paired PNA strands, which co-locates the reactive Fe/NTA groups to this position.

Thus, $PDII^{12}$ and $PDIII^{12}$ are structurally different. The $PDII^{12}$ complex exhibit optimal strand polarity at the expense of a reduced number of base pairs (only 7 out of 12 possible invasion base pairs), whereas $PDIII^{12}$ complex has compromised strand polarity (parallel Watson–Crick base-paired PNA strand) but an optimal number of base pairs (12 invasion base pairs).

Pentadecamer PNA–dsDNA complexes

As suggested by the increase in product complexity on going from PNA decamer to PNA dodecamer, the number

of PNA–dsDNA complexes increased even further when using the PNA pentadecamer now counting at least 7 complexes: PDI^{15}–$PDVII^{15}$ (Figure 3). In analogy to the results for the PNA dodecamer, the distribution among the pentadecamer PNA–dsDNA complexes is highly PNA concentration dependent (Figure 3A) and sensitive to ionic strength (Figure 3B): PDI^{15}–$PDII^{15}$ and $PDIII^{15}$–$PDVII^{15}$ are prominent at low and high PNA concentrations, respectively. On increasing the ionic strength, PDI^{15} and $PDII^{15}$ appear at the expense of $PDIII^{15}$–$PDVII^{15}$. This suggests that PDI^{15} and $PDII^{15}$ represent triplex type structures whereas $PDIII^{15}$ through $PDVII^{15}$ most likely correspond to various distinct invasion complexes.

DMS probing of gel-excised complexes PDI^{15} and $PDII^{15}$ showed protection of all target guanines (G_6 through G_{14}; Figure 3C, lanes 3 and 4) and $KMnO_4$ probing revealed resistance to oxidation of all target thymines (T_1–T_{15}; Figure 3D, lanes 3 and 4) consistent with these complexes being triplex type structures containing a single PNA strand bound via Hoogsteen base pairs to the DNA target. These data could be compatible with the existence of two triplexes, one with the PNA bound parallel to the entire target (A_1–A_{15}), and another with the PNA bound anti-parallel to only part of the target (A_5–A_{15}). However, Fe/NTA affinity cleavage unambiguously establishes that the PNA strand bound via Hoogsteen base pairs is hybridized to the DNA target in a parallel orientation for both complexes (Figure 3C, lanes 2 and 3).

Enigmatically, complexes PDI^{15} and $PDII^{15}$ are clearly different structures as based on their electrophoretic mobility differences in native gels (Figure 3A and B)—yet they are indistinguishable via chemical probing, at least using the present methods. This result could, in principle, be caused by an inhomogeneous PNA oligomer preparation containing truncated or modified PNA molecules. However, although small amounts of impurities were seen by HPLC, mass spectrometry revealed only a single peak of the correct mass arguing against this (data not shown). Furthermore, since PDI^{15} and $PDII^{15}$ show similar affinity cleavage intensities (Figure 3E), both complexes must contain full-lenth PNA oligomers because the NTA group is conjugated to the PNA oligomer in the last coupling step.

Chemical probing of gel-excised $PDVI^{15}$ (i.e. in fact two poorly resolved complexes) and $PDVII^{15}$ revealed that both complexes show protection towards DMS methylation of all DNA target guanines (G_6 through G_{14}; Figure 3C, lanes 7 and 8). Thus both complexes contain a PNA strand bound via Hoogsteen base pairs to at least part of the target, but most likely to the entire target (A_1 through A_{15}). Although the Fe/NTA affinity cleavage yielded inconclusive data for invasion complexes involving PNA pentadecamer due to interference with gel-mobility by the exceedingly stable PNA_2–DNA triplex (data not shown), we favour a structure in which the Hoogsteen base-paired PNA strand binds parallel to the target DNA strand because this is observed in the case of all PD^{12} complexes as well as for PDI^{15} and $PDII^{15}$, and is the preferred orientation for PNA Hoogsteen hybridization (18).

As in the case of $PDII^{12}$ and $PDIII^{12}$, probing of gel-excised $PDVI^{15}$ and $PDVII^{15}$ revealed notable differences in hypersensitivity to permanganate oxidation of target thymines (Figure 3D). In the case of $PDVI^{15}$, target residues T_1 through T_4 showed minimal reactivity, T_5 exhibit intermediate hypersensitivity, and T_7–T_{15} were all strongly reactive towards permanganate. These results are consistent with partial invasion by a PNA strand bound via Watson–Crick base pairs to target residues A_7 through $A_{15,}$ most likely in an anti-parallel orientation. Permanganate probing of the $PDVII^{15}$ complex revealed strong and almost equal hypersensitivity along the entire DNA target compatible with invasion of the target by a PNA strand bound to the entire target (A_1 through A_{15}) in a parallel orientation.

Thus $PDVI^{15}$ and $PDVII^{15}$ are distinct structures. Most likely, both complexes have a fully hybridized parallel Hoogsteen base-paired PNA strand (i.e. bound to residues A_1–A_{15}). $PDVI^{15}$ has a reduced number of Watson–Crick base pairs (9 out of 15 bp), presumably reflecting an optimal binding orientation of the invasion PNA strand. In contrast, $PDVII^{15}$ has an optimal number of Watson–Crick base-pairs, which can only take place with suboptimal PNA strand polarity. In other words, $PDVII^{15}$ appears to be a conventional P-loop structure with a 15 bp internal PNA–DNA–PNA triple helix and a corresponding stretch of displaced DNA, whereas $PDVI^{15}$, due to an internal duplex–triplex hybrid shows only ~9–10 bp of looped out DNA (Figure 3F).

The least prominent complexes $PDIII^{15}$ through PDV^{15} remain incompletely understood in part because $PDIV^{15}$ and PDV^{15} could not be separated. Consequently, specific structural assignments have been omitted for these complexes and the probing data are merely summarized (Figure 3F, $PDIII^{15}$ or $PDIV^{15}$/PDV^{15}). Probing of gel-excised $PDIII^{15}$ or the $PDIV^{15}$/PDV^{15} mixture showed that these different complexes have in common that all target guanine residues except G_{14} (the 3′-ultimate guanine) show protection towards DMS methylation indicating that a PNA strand binds incompletely to the target sequence via Hoogsteen base pairs (Figure 3C, lanes 5 and 6). Further chemical probing of $PDIII^{15}$ and $PDIV^{15}$/PDV^{15} revealed maximal permanganate hypersensitivity in the middle of the target (T_7 through T_{12}). Towards the 3′ end of the target of both $PDIII^{15}$ and $PDIV^{15}$/PDV^{15} showed reduced hypersensitivity towards $KMnO_4$ at position T_{15}. Towards the 5′ end of the target, $PDIII^{15}$ and $PDIV^{15}$/PDV^{15} differed with respect to permanganate reactivity. $PDIII^{15}$ showed only marginal reactivity at residues T_1 through T_4 and intermediate hypersensitivity at position T_5. The $PDIV^{15}$/PDV^{15}, however, showed minimal permanganate reactivity at position T_1 and T_2 and intermediate hypersensitivity at positions T_3–T_5. Thus $PDIII^{15}$ and $PDIV^{15}$/PDV^{15} are clearly distinct structures with respect to the helix invasion PNA strand. Together these results show that stable invasion complexes involving structures with incompletely bound Hoogsteen and/or Watson–Crick base-paired PNA strands can result upon binding of a PNA pentadecamer to a cognate dsDNA target.

Conversion of triplex to invasion complex

Previous studies have addressed the mechanism of PNA helix invasion of a dsDNA target suggesting the triplex as an intermediate (23,25,26). The present results reveal distinct and stable triplex structures (Figures 2 and 3), and therefore it should be possible to study their possible interconversion

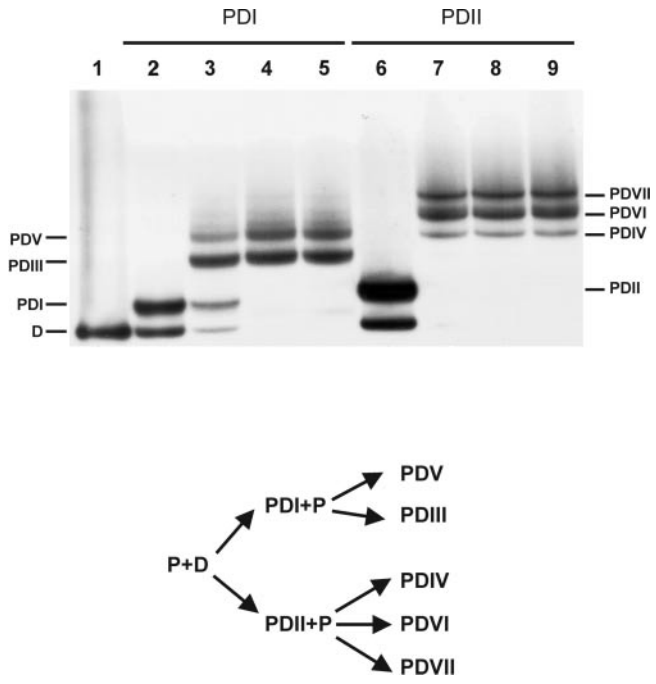

Figure 4. Chasing isolated PD[15] triplexes into structurally distinct invasion complexes. Upper panel: Autoradiograph showing conversion of triplex to invasion complex. The triplexes PDI[15] and PDII[15] were generated using 6 μM PNA1940 and isolated by excision and crushing of the gel-slices. PDI[15] (lanes 2–5) and PDII[15] (lanes 6–9) were incubated with fresh PNA1940 in the gel-slurry and resolved by gel-shift analysis. The following PNA concentrations were used: w/o (lanes 1, 2 and 6), 1 μM (lanes 3 and 7), 3 μM (lanes 4 and 8) and 6 μM (lanes 5 and 9). The PDI[15] triplex is transformed into the invasion species PDIII[15] and PDV[15] whereas PDII[15] is chased into PDIV[15], PDVI[15] and PDVII[15]. The 168 bp XbaI–PvuII restriction fragment of p322 5′-kinase labeled with ^{32}P-phosphate at the XbaI site was used. Lower panel: Diagram showing the relationship between complexes. PNA incubations were carried out at pH 6.5.

and conversion into invasion complexes by incubation of isolated triplex with additional PNA oligomer. Hence gel-purified PDI[15] and PDII[15] triplexes were challenged with additional PNA pentadecamer (Figure 4). Indeed, PDI[15] and PDII[15] were transformed into various new species. Surprisingly, each specific triplex yielded unique invasion complexes: PDI[15] produced PDIII[15] and PDV[15] while PDII[15] gave rise to PDIV[15], PDVI[15] and PDVII[15] (Figure 4). Furthermore, the two triplexes PDI[15] and PDII[15] were not interconvertible. These results provide compelling evidence that a triplex is indeed a substrate for invasion and also supports that the triplexes PDI[15] and PDII[15] are structurally different. Irrespective of the nature of this difference and of its cause, each triplex produces a distinct family of invasion complexes indicating that binding of the 'Watson–Crick' PNA strand occurs via the pre-existing 'Hoogsteen type' triplex—and does not require or promote its dissociation. We also note that base pair alterations apparently take place in the Hoogsteen base-paired-PNA strand upon transformation from PDI[15] to PDIII[15] (Figure 3C, cf. lanes 3 and 5) (see below).

Kinetics

Further investigation of the conversion of triplex to invasion complexes was done by monitoring the time course of the

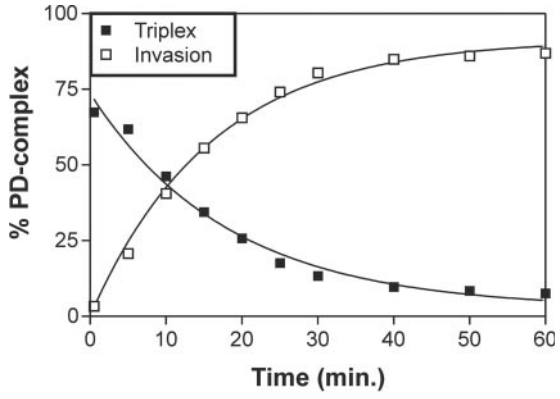

Figure 5. Kinetic analysis of triplex and invasion complex formation. Amount of triplex or invasion complex as a function of time. PNA–dsDNA complex formation was conducted using PNA1940 followed by gel-shift and phosphorimaging analysis. The 168 bp XbaI–PvuII restriction fragment of p322 was used 3′-Klenow labeled with ^{32}P-phosphate as described in Materials and Methods.

reactions in a low ionic strength buffer (Figure 5). The triplex is formed very rapidly and the amount of this complex reaches its maximal value already at the first time point (30 s), and then diminishes as invasion complexes emerge (Figure 5). A control experiment in which surplus of an oligonucleotide complementary to the PNA was added at 30 s of incubation completely inhibited the formation of invasion complexes presumably by trapping free PNA. In contrast, the amount of triplex produced at this time point remained constant over the entire experiment indicating no dissociation of this complex (data not shown). Therefore, these results confirm that a direct transformation of a PNA–dsDNA 'Hoogsteen' type triplex into a PNA–DNA–PNA, DNA invasion complex does indeed take place.

Although the investigated triplexes are stable in the absence of excess PNA oligomer, the base-pair alterations of the Hoogsteen PNA strand observed upon transformation of PDI[15] to PDIII[15] suggest that remodelling of the Hoogsteen PNA strand may take place upon helix invasion by a Watson–Crick binding PNA strand.

The experiments in this study were performed at slightly acidic pH to facilitate protonation of cytosine N3. To demonstrate that the results extend to a physiologically relevant pH, an analogous experiment was carried out at pH 7.3 using a pentadecamer homopyrimidine PNA oligomer containing pseudoisocytosine (18) instead of cytosine. Binding of this PNA to the target gave rise to a multitude of complexes analogously to what was observed for the corresponding cytosine PNA (Supplementary Figure S2). Moreover, the results underline that the specific complexes formed as well as their migration in the gel depend on the specific PNA oligomer used. In particular, the sequence will of course dictate which complexes are stable, but other chemical modification (such as charge) may also be of importance.

CONCLUSION

The first conclusion drawn from the present work is that extending the strand length of homopyrimidine PNA

oligomers increases the structural heterogeneity of resulting sequence targeted PNA–dsDNA complexes and this increased product complexity is due to the formation of kinetically trapped (but thermodynamically suboptimal) complexes involving compromised PNA strand orientation and incomplete base pairing. Thus, target selectivity of helix invasion is expected to be reduced when addressing longer than decamer sequences because kinetically stable complexes that do not involve recognition of the entire target can be formed. Indeed, we observe only limited differences of binding efficiency when targeting decamer, dodecamer and pentadecamer dsDNA targets by a pentadecamer homopyrimidine PNA via helix invasion (unpublished data). Such extended dsDNA sequences may, however, be targeted using modular constructs containing PNA oligomer conjugated to small molecule DNA binding agents such as the minor groove binder Hoechst (39). In this approach, the sequence preference of the minor groove binder selects a subset of targets via equilibrium interactions with its own target, which is followed by PNA helix invasion at sites that contain an adjacent PNA target.

It is important to emphasize that the binding diversity and target discrimination described for the PNA oligomers is a consequence of kinetic control and not of thermodynamic equilibrium because of the very high stability and thus long life times of the complexes (40). This is analogous to the trapping of meta-stable intermediates in RNA folding (41) as well as protein folding (42), which can result in incorrectly folded and dysfunctional structures. In most protein–DNA interactions, the affinity has been tuned by evolution (perhaps to avoid this type of kinetic trapping) such that sequence specificity is controlled by thermodynamics.

The second conclusion is that it is possible to stably target single sites in dsDNA via a triplex strategy when using homopyrimidine PNA oligomers longer than 12mer. Previous investigations have reported the formation of triplexes between PNA oligomers and complementary dsDNA targets (26,43) but so far there has been no structural characterization of such complexes. Detailed studies addressing the specificity and affinity of such PNA–dsDNA triplex interactions are under way in order to explore whether this approach has advantages over other triplex targeting strategies (3,4).

The third conclusion from the present work is that a stable non-invasion 'Hoogsteen type' triplex homopyrimidine PNA–dsDNA intermediate can be directly converted into a helix invasion P-loop complex involving combined Hoogsteen and Watson–Crick base pairs. Thus the 'Hoogsteen first' mechanism is valid at least for the employed pentadecamer under the present conditions. However, we are not able to conclude that this is the general mechanism for triplex invasion, since PNA sequence (especially C-content) and strand length as well as template topology and dynamics (e.g. resulting from the activity of DNA processing enzymes) may alter the mechanism of P-loop formation.

ACKNOWLEDGEMENTS

This work is supported by the Danish Medical Research Council (grant no.: 22-04-0456), the Novo Nordisk Foundation and the EU commission (SNIPER contract no.: LSHB-CT-2004-005204). Funding to pay the Open Access publication charges for this article was provided by EU commission.

Conflict of interest statement. None declared.

REFERENCES

1. Porteus,M.H. and Carroll,D. (2005) Gene targeting using zinc finger nucleases. *Nat. Biotechnol*., **8**, 967–973.
2. Dervan,P.B., Doss,R.M. and Marques,M.A. (2005) Programmable DNA binding oligomers for control of transcription. *Curr. Med. Chem. Anticancer Agents*, **4**, 373–387.
3. Rogers,F.A., Lloyd,J.A. and Glazer,P.M. (2005) Triplex-forming oligonucleotides as potential tools for modulation of gene expression. *Curr. Med. Chem. Anticancer Agents*, **5**, 319–326.
4. Besch,R., Giovannangeli,C. and Degitz,K. (2004) Triplex-forming oligonucleotides—sequence-specific DNA ligands as tools for gene inhibition and for modulation of DNA-associated functions. *Curr. Drug Targets*, **8**, 691–703.
5. Bentin,T., Larsen,H.J. and Nielsen,P.E. (2004) Peptide nucleic acid targeting of double stranded DNA. In Nielsen (ed.), *Peptide Nucleic Acids: Protocols and Applications*, 2nd edn. Horizon Bioscience, Norfolk England, pp. 107–140.
6. Kaihatsu,K., Janowski,B.A. and Corey,D.R. (2004) Recognition of chromosomal DNA by PNAs. *Chem. Biol*., **11**, 749–758.
7. Nielsen,P.E., Egholm,M., Berg,R.H. and Buchardt,O. (1991) Sequence-selective recognition of DNA by strand displacement with a thymine-substituted polyamide. *Science*, **254**, 1497–1500.
8. Egholm,M., Buchardt,O., Christensen,L., Behrens,C., Freier,S.M., Driver,D.A., Berg,R.H., Kim,S.K., Nordén,B. and Nielsen,P.E. (1993) PNA hybridizes to complementary oligonucleotides obeying the Watson-Crick hydrogen-bonding rules. *Nature*, **365**, 556–568.
9. Nielsen,P.E., Egholm,M. and Buchardt,O. (1994) Evidence for $(PNA)_2$/DNA triplex structure upon binding of PNA to dsDNA by strand displacement. *J. Mol. Recognit*., **7**, 165–170.
10. Hanvey,J.C., Peffer,N.J., Bisi,J.E., Thomson,S.A., Cadilla,R., Josey,J.A., Ricca,D.J., Hassman,C.F., Bonham,M.A., Au,K.G. *et al*. (1992) Antisense and antigene properties of peptide nucleic acids. *Science*, **258**, 1481–1485.
11. Pfeffer,N.J., Hanvey,J.C., Bisi,J.E., Thomson,S.A., Hassman,C.F., Noble,S.A. and Babiss,L.E. (1993) Strand-invasion of duplex DNA by peptide nucleic acid oligomers. *Proc. Natl Acad. Sci. USA*, **90**, 10648–10652.
12. Nielsen,P.E., Egholm,M. and Buchardt,O. (1994) Sequence-specific transcription arrest by peptide nucleic acid bound to the DNA template strand. *Gene*, **149**, 139–145.
13. Vickers,T.A., Griffith,M.C., Ramasmay,K., Risen,L.M. and Freier,S.M. (1995) Inhibition of NF-kappa B specific transcriptional activation by PNA strand invasion. *Nucleic Acids Res*., **23**, 3003–3008.
14. Larsen,H.J. and Nielsen,P.E. (1996) Transcription-mediated binding of peptide nucleic acid (PNA) to double-stranded DNA: sequence-specific suicide transcription. *Nucleic Acids Res*., **24**, 458–463.
15. Liu,B., Han,Y., Ferdous,A., Corey,D.R. and Kodadek,T. (2003) Transcription activation by a PNA-peptide chimera in a mammalian cell extract. *Chem. Biol*., **10**, 909–916.
16. Møllegaard,N.E., Buchardt,O., Egholm,M. and Nielsen,P.E. (1994) Peptide nucleic acid-DNA strand displacement loops as artificial transcription promoters. *Proc. Natl Acad. Sci. USA*, **91**, 3892–3895.
17. Wang,G., Xu,X., Pace,B., Dean,D.A., Glazer,P.M., Chan,P., Goodman,S.R. and Shokolenko,I. (1999) Peptide nucleic acid (PNA) binding-mediated induction of human gamma-globin gene expression. *Nucleic Acids Res*., **27**, 2806–2813.
18. Egholm,M., Christensen,L., Dueholm,K.L., Buchardt,O., Coull,J. and Nielsen,P.E. (1995) Efficient pH-independent sequence-specific DNA binding by pseudoisocytosine-containing bis-PNA. *Nucleic Acids Res*., **23**, 217–222.
19. Griffith,M.C., Riesen,L.M., Greig,M.J., Lesnik,E.A., Sprankle,K.G., Griffey,R.H., Kiely,J.S. and Freier,S.M. (1995) Single and bis peptide nucleic acids as triplexing agents: binding and stoichiometry. *J. Am. Chem. Soc*., **117**, 831–832.

20. Bentin,T. and Nielsen,P.E. (2003) Superior duplex DNA strand invasion by acridine conjugated peptide nucleic acids. *J. Am. Chem. Soc*., **125**, 6378–6379.
21. Hansen,G.I., Bentin,T., Larsen,H.J. and Nielsen,P.E. (2001) Structural isomers of bis-PNA bound to a target in duplex DNA. *J. Mol. Biol*., **307**, 67–74.
22. Kosaganov,Y.N., Stetsenko,D.A., Lubyako,E.N., Kvito,N.P., Lazurkin,Y.S. and Nielsen,P.E. (2000) Effect of temperature and ionic strength on the dissociation kinetics and lifetime of PNA-DNA triplexes. *Biochemistry*, **39**, 11742–11747.
23. Demidov,V.V., Yavnilovich,M.V., Belotserkovskii,B.P., Frank-Kamenetskii,M.D. and Nielsen,P.E. (1995) Kinetics and mechanism of polyamide ('peptide') nucleic acid binding to duplex DNA. *Proc. Natl Acad. Sci. USA*, **92**, 2637–2641.
24. Kuhn,H., Demidov,V.V., Frank-Kamenetskii,M.D. and Nielsen,P.E. (1998) Kinetic sequence discrimination of cationic bis-PNAs upon targeting of double-stranded DNA. *Nucleic Acids Res*., **26**, 582–587.
25. Kuhn,H., Demidov,V.V., Nielsen,P.E. and Frank-Kamenetskii,M.D. (1999) An experimental study of mechanism and specificity of peptide nucleic acid (PNA) binding to duplex DNA. *J. Mol. Biol*., **286**, 1337–1345.
26. Zhilina,Z.V., Ziemba,A.J., Nielsen,P.E. and Ebbinghaus,S.W. (2006) PNA-nitrogen mustard conjugates are effective supressors of HER-2/neu and biological tools for recognition of PNA/DNA interactions. *Bioconjug. Chem*., **17**, 214–222.
27. Christensen,L., Fitzpatrick,R., Gildea,B., Petersen,K.H., Hansen,H.F., Koch,T., Egholm,M., Buchardt,O., Nielsen,P.E., Coull,J. and Berg,R.H. (1995) Solid-phase synthesis of peptide nucleic acids. *J. Peptide Sci*., **3**, 175–183.
28. Lohse,J., Hui,C., Sönnichsen,S.H. and Nielsen,P.E. (1996) Sequence selective DNA cleavage by PNA-NTA conjugates. In Meunier,B. (ed.), *DNA and RNA Cleavers and Chemotherapy of Cancer and Viral Diseases*. Kluwer Academic Publishers, pp. 133–141.
29. Sambrook,J. and Russel,D.W. (2001) *Molecular Cloning: A laboratory manual, 3rd edn*. Cold Spring Harbor Laboratory Press, NY.
30. Bukanov,N.O., Demidov,V.V., Nielsen,P.E. and Frank-Kamenetskii,M.D. (1998) PD-loop: a complex of duplex DNA with an oligonucleotide. *Proc. Natl Acad. Sci. USA*, **95**, 5516–5520.
31. Rubin,C.M. and Schmid,C.W. (1988) Pyrimidine-specific chemical reactions useful for DNA sequencing. *Nucleic Acids Res*., **8**, 4613–4619.
32. Maxam,A.M. and Gilbert,W. (1977) A new method for sequencing DNA. *Proc. Natl Acad. Sci. USA*, **74**, 560–564.
33. Bentin,T., Larsen,H.J. and Nielsen,P.E. (2003) Combined triplex/duplex invasion of double–stranded DNA by 'tail-clamp' peptide nucleic acid. *Biochemistry*, **42**, 13987–13995.
34. Cherny,D.Y., Belotserkovskii,B.P., Frank-Kamenetskii,M.D., Egholm,M., Buchardt,O., Berg,R.H. and Nielsen,P.E. (1993) DNA unwinding upon strand-displacement binding of a thymine-substituted polyamide to double-stranded DNA. *Proc. Natl Acad. Sci. USA*, **90**, 1667–1670.
35. Bentin,T. and Nielsen,P.E. (1996) Enhanced peptide nucleic acid binding to supercoiled DNA: possible implications for DNA 'breathing' dynamics. *Biochemistry*, **35**, 8863–8869.
36. Kurakin,A., Larsen,H.J. and Nielsen,P.E. (1998) Cooperative strand displacement by peptide nucleic acid (PNA). *Chem. Biol*., **5**, 81–89.
37. Arimondo,P.B. and Helene,C. (2001) Design of new anti-cancer agents based on topoisomerase poisons targeted to specific DNA sequences. *Curr. Med. Chem. Anticancer Agents*, **3**, 219–235.
38. Moser,H.E. and Dervan,P.B. (1987) Sequence-specific cleavage of double helical DNA by triple helix formation. *Science*, **238**, 645–650.
39. Nielsen,P.E., Frederiksen,K. and Behrens,C. (2005) Extended target sequence specificity of PNA-minor-groove binder conjugates. *Chembiochem*, **6**, 66–68.
40. Demidov,V.V. and Frank-Kamenetskii,M.D. (2004) Two sides of the coin: affinity and specificity of nucleic acid interactions. *Trends Biochem. Sci*., **29**, 62–71.
41. Schroeder,R., Barta,A. and Semrad,K. (2004) Strategies for RNA folding and assembly. *Nature Rev. Mol. Cell Biol*., **5**, 908–919.
42. Thirumalai,D. and Hyeon,C. (2005) RNA and protein folding: common themes and variations. *Biochemistry*, **44**, 4957–4970.
43. Wittung,P., Nielsen,P. and Norden,B. (1997) Extended DNA-recognition repertoire of peptide nucleic acid (PNA): PNA-dsDNA triplex formed with cytosine-rich homopyrimidine PNA. *Biochemistry*, **36**, 7973–7979.